EARTH SURFACE PROCESSES AND LANDFORMS
Earth Surf. Process. Landforms (2020)
© 2020 John Wiley & Sons, Ltd.
Published online in Wiley Online Library
(wileyonlinelibrary.com) DOI: 10.1002/esp.5017

Seven decades of hydrogeomorphological changes in a near-natural (Sense River) and a hydropower-regulated (Sarine River) pre-Alpine river floodplain in Western Switzerland

Diego Tonolla,[1,2]* Martin Geilhausen[3] and Michael Doering[1,2]
[1] Institute of Natural Resource Sciences, Zurich University of Applied Sciences (ZHAW), Grüental, Wädenswil, Switzerland
[2] eQcharta GmbH, Wädenswil, Switzerland
[3] Department of Structural Engineering, GIS Competence Centre, Zurich, Switzerland

Received 4 March 2020; Revised 21 September 2020; Accepted 24 September 2020

*Correspondence to: Diego Tonolla, Institute of Natural Resource Sciences, Zurich University of Applied Sciences (ZHAW), Grüental, 8820 Wädenswil, Switzerland.
E-mail: diego.tonolla@zhaw.ch

ESPL
Earth Surface Processes and Landforms

ABSTRACT: Hydropower alteration of the natural flow and sediment regime can severely degrade hydromorphology, thereby threatening biodiversity and overall ecosystem processes of rivers and their floodplains. Using sequences of aerial images, we quantified seven decades (1938/1942–2013) of spatiotemporal changes in channel and floodplain morphology, as well as changes in the physical habitats, of three floodplain river reaches of the Swiss pre-Alps, two hydropower-regulated and one near-natural. In the Sarine River floodplain, within the first decades of hydropower impairment, the magnitude and frequency of flood events (Q_2, Q_{10}, Q_{30}) decreased substantially. As a result, the area of pioneer floodplain habitats that depend on flood activity and sediment dynamic, such as bare sediments, decreased dramatically by approximately 95%. However, by 2013 vegetated areas had generally increased in comparison to the pre-regulation period in 1943, indicating general vegetative colonization. Between 1943 and 2013, the active channel underwent essential narrowing (up to 62% width reduction in the residual flow reach) and habitat turnover rates were very low (5% of the total floodplain area changed habitat type five to six times). In contrast, from the 1950s onwards, the near-natural floodplain of the Sense River experienced recurrent narrowing and widening, and frequent changes between bare and vegetated areas, reflecting the shifting habitat mosaic concept typical for natural floodplains. In the three reaches investigated, we found that the active floodplain width and erosion of vegetated areas were primarily controlled by medium to large floods (Q_{10}, Q_{30}), which combined with reduced time intervals between ordinary floods $\geq Q_2$ most likely mobilized streambed sediments and limited the ability of vegetation to establish itself on bare gravel bars within the parafluvial zone. These findings can contribute to restoration action plans such as controlled flooding and sediment replenishments in the Sarine and other floodplain rivers of the Alps.
© 2020 John Wiley & Sons, Ltd.

KEYWORDS: hydropower impacts; river and floodplain restoration; altered flow and sediment regime; aerial image analyses; geomorphic changes; active floodplain

Introduction

Hydropower is an important renewable energy source with excellent efficiency, currently accounting (excluding pumped storage) for approximately 16% of the world's electricity generation (IEA, 2018) and approximately 57% in Switzerland (SFOE, 2019). Even though most of these hydropower facilities provide important benefits to human societies and their economies, they may have detrimental impacts on downstream river ecosystems by altering the natural equilibrium between flow and sediment regime (Poff *et al.*, 1997; Wohl *et al.*, 2015a). The upstream and downstream propagation of fragmentation and flow regulation caused by dams and reservoirs are considered to be the dominant factors that disrupt river connectivity (Grill *et al.*, 2019). High-head hydropower dams affect flow dynamics, often releasing only a low flow (also called base or residual flow) lacking natural flood–drought cycles (Poff *et al.*, 1997; Richter *et al.*, 2003). Further, downstream of hydroelectric power plants, rivers may also exercise unnatural daily or sub-daily quick variations in discharge and water levels (i.e. hydropeaking; Moog, 1993; Meile *et al.*, 2011) at a rate that varies in response to turbine operations according to the demand of the electricity market. Thus alteration of the flow and sediment regime by hydropower facilities often severely affects hydrogeomorphological variability and dynamics, which in turn support biota (especially disturbance-adapted aquatic and riparian communities) and overall ecosystem processes (e.g. production, transformation and storage of organic matter and nutrients) of rivers and their floodplains (Bunn and Arthington, 2002; Graf, 2006; Poff *et al.*, 2007; Poff and

Zimmermann, 2010; Vörösmarty *et al.*, 2010; Best, 2019; Palmer and Ruhi, 2019; and references therein).

Unregulated river floodplains are complex, dynamic and diverse ecosystems characterized by interconnected aquatic and terrestrial habitat patches. These patches are generated and maintained by frequent expansion–contraction cycles of surface waters, channel avulsion and cut-and-fill alluviation, mainly as a result of variability in flow, and flood pulses and sediment regime in interaction with riparian and in-channel vegetation (Tockner and Stanford, 2002; Ward *et al.*, 2002; Tockner *et al.*, 2010a; Gurnell, 2014; and references therein). Moreover, floodplains are one of the most vulnerable and threatened ecosystems worldwide (Tockner and Stanford, 2002; Tockner *et al.*, 2010b). Their pronounced heterogeneity over a wide range of temporal and spatial scales and frequent habitat turnover occur much more rapidly than in most other ecosystems, distinguishing them as excellent model ecosystems (Tockner *et al.*, 2010a) to study the impact of hydropower exploitations on the spatiotemporal organization of channel and floodplain morphology including physical habitat variability.

Sequences of remotely sensed aerial images are frequently used to digitize surface areas in order to identify changes in physical habitats at the reach scale over decades, and are therefore essential in the analysis and management of river systems (Grabowski *et al.*, 2014; Belletti *et al.*, 2017). Nevertheless, remotely sensed data are limited to a snapshot in time and should, whenever possible, be combined with other data sources and observations. In French river systems, they have been successfully used to determine the role of flood activity and bedload supply in controlling channel width, vegetation dynamics and island patterns in both braided (Belletti *et al.*, 2014, 2015) and bedrock alluvial (Toone *et al.*, 2014) reaches. Moreover, historical aerial image analyses have been used to identify spatiotemporal changes in habitat proportion and variability in a Swiss alpine floodplain affected by water abstraction and levee constructions (Doering *et al.*, 2012), and within two alluvial reaches of a Mediterranean river located downstream of large dams (Garófano-Gómez *et al.*, 2013). Further, aerial images have been combined with historical maps (Hohensinner *et al.*, 2011) or airborne LiDAR (Lallias-Tacon *et al.*, 2017) to characterize the history of river floodplain morphology, development of habitats and vegetation responses. Overall, these studies suggest that flow and sediment regulation generally lead to active channel (AC) incision and narrowing with consequent disconnection from former AC or active floodplain (AF) areas as well as to increased channel and floodplain stabilization through changes in vegetation composition (i.e. pioneer versus mature vegetation) and encroachment.

The main goal of our study was to quantify seven decades of spatiotemporal transformation of channel and floodplain morphology, including physical habitat turnover, in near-natural and hydropower-regulated river floodplains of the Swiss pre-Alps. We analysed a series of aerial images extending over a period of 70–75 years relating to two river reaches characterized by a residual flow and hydropeaking regime. Both reaches are connected downstream and affected by hydropower facilities (dam, hydropower plant). Equivalent analyses were performed for a floodplain reach with a near-natural flow and sediment regime in an adjacent catchment, serving as comparison. We expected that modification of the natural flow and sediment regime in the two hydropower-affected reaches would change habitat proportion as well as distribution, and increase morphological stability as a consequence of promoted vegetation succession. Our study aims at quantifying long-term trajectories of changes, using and specifying several variables to better assess consequences of persisting hydropower pressures and resulting hydrogeomorphological responses over decades in floodplains. It also aims at supporting sustainable restoration and adaptive management strategies in hydropower-regulated rivers and floodplains.

Study Sites

Three different floodplain reaches of national importance, i.e. protected areas, located in alluvial zones of two Swiss pre-alpine rivers were selected for spatiotemporal quantification of morphological changes by means of aerial image analyses (Figure 1 and Table 1). The Sarine River is 126 km long and drains a catchment of 1893 km^2 before flowing into the Aare River, a tributary of the Rhine River (Mapgeo, 2020). On its course, the Sarine is exploited for hydroelectrical production in five facilities that impair its flow and sediment regime. Between the Rossens dam (Lake Gruyère) and the Maigrauge dam (Lake Pérolles) the meandering course of the river is well developed and constrained in a 50–100 m deep canyon in the Miocene molasses bedrock (Braillard and Mauvilly, 2008). The investigated 11 km long residual flow reach (henceforth, Sarine-Residual) was located between 2.4 km downstream of the Rossens dam and the hydropower plant Hauterive (Figure 1 and Table 1). The 6.5 km long hydropeaking reach (henceforth, Sarine-Hydropeaking) was located between the water release of the hydropower plant Hauterive and 1.7 km upstream of the Maigrauge dam (Figure 1 and Table 1). The Sense originates at the confluence of the Cold and Warm Sense and drains a catchment of 435 km^2 before joining the Sarine after 36 km (Mapgeo, 2020). The Sense is one of the most natural rivers in the northern Alpine region (Hettrich *et al.*, 2011). The investigated 3.5 km braided floodplain reach was located near the village of Plaffeien and characterized by a near-natural flow and sediment regime (Figure 1 and Table 1), only slightly constrained by former gravel extraction and some levees installed for flood protection and bank stabilization in the 1950s. Average total annual rainfall in the Sarine (station Fribourg-Posieux) and Sense (station Guglera) reaches is 1075 and 1345 mm, with average maximum and minimum monthly rainfall typically occurring in August and in February, respectively (period 1920–2016; MeteoSwiss, 2017).

Historical changes in flow and sediment regime

The Rossens dam was built from 1944 to 1948 (arch dam height 83 m; crest length 320 m; Gigot, 1950) forming Lake Gruyère, the longest (~13 km) and fourth largest (170–200 × 10^6 m^3) Swiss reservoir. After the construction of the Rossens dam the hydropower plant Hauterive, built between 1898 and 1901, was renewed and connected with the reservoir by a ~6 km long circular gallery (Gigot, 1950) for on-demand turbine operation, resulting in hydropeaking downstream. Currently, the mean annual production is 220 GW h and the maximum discharge through the gallery is 84 m^3 s^{-1}. The actual residual flow between the Rossens dam and Hauterive varies between 2.5 and 3.5 m^3 s^{-1} in winter and summer, respectively. However, because of renewals of the hydropower facilities, the residual flow and hydropeaking regime in the two Sarine reaches have changed considerably over the years (Table 2). The Sense reach is not affected by hydropower facilities.

The discharge at the hydrological station 'Fribourg' (located ~10 km downstream of the hydropower plant Hauterive; FOEN, 2020) is influenced by the Maigrauge dam (hydropower plant Oelberg; Q_{max} = 99 m^3 s^{-1}, since 1956) and the two main

© 2020 John Wiley & Sons, Ltd.

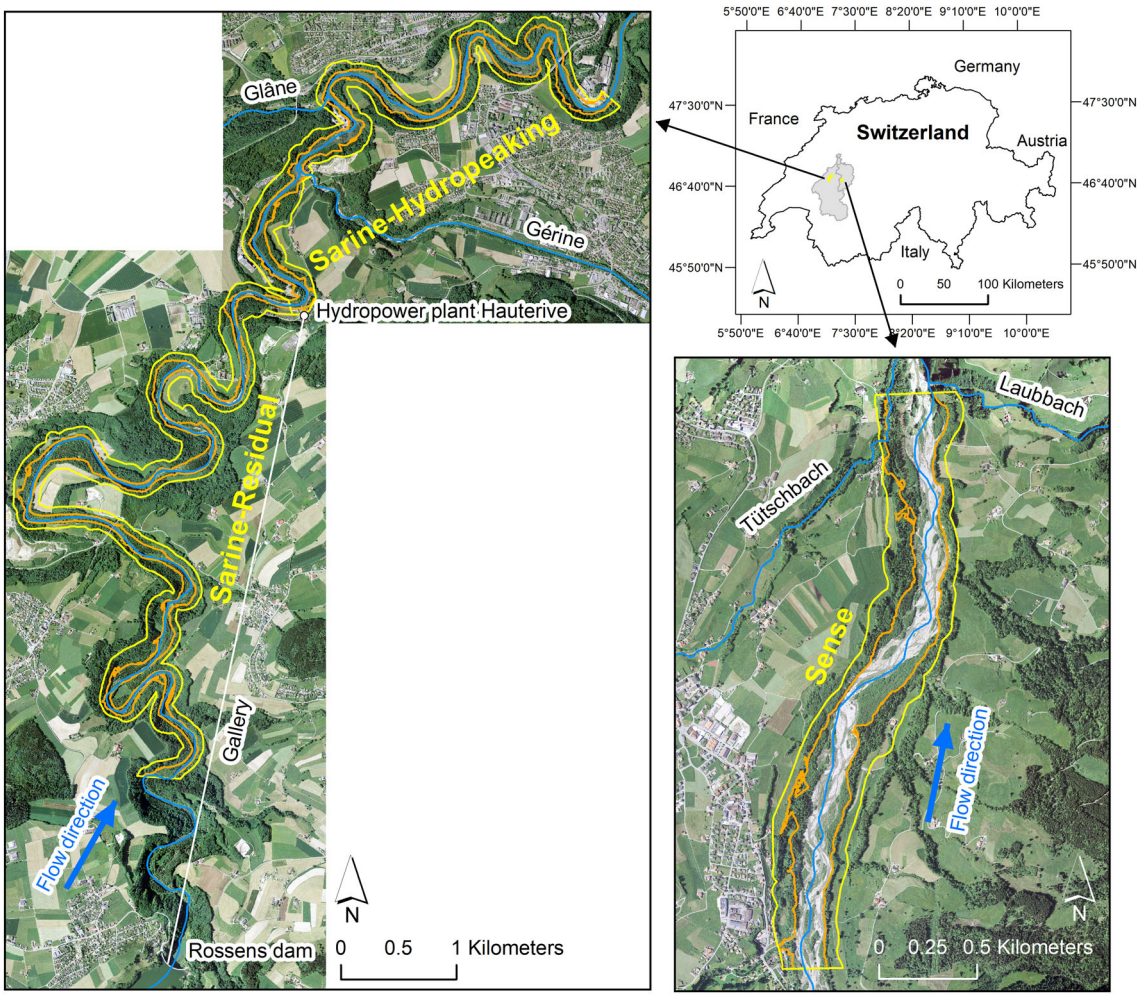

Figure 1. Overview of the three study reaches: Sarine-Residual, Sarine-Hydropeaking, and Sense (near-natural). Major hydropower facilities (Rossens dam, gallery and hydropower plant Hauterive) and tributaries are indicated. Yellow polygons illustrate the reach boundaries and orange polygons the maximum active floodplain area (see text: 'Habitat delimitation' and 'Floodplain and habitat variables, flood variables'). Background maps: orthophotos of the year 2013 (Swissimage Geodata Swisstopo©).

Table 1. Characterization of the study reaches in their actual state

	Sarine-Residual	Sarine-Hydropeaking	Sense
Strahler's order	7	7	6
Valley confinement and floodplain planform[a]	Partly confined, single-thread meandering		Laterally unconfined, multi-thread braided
Average channel slope (‰)	3	2	17
Sediment size D_m|D_{90} (cm)	5.6|11		9.6|22
Main channel average width (m)	25	50	10
Mean elevation (m a.s.l.)	590	560	810
Source elevation (m a.s.l.)	2250		1500[b]
Natural flow regime	Intermediate nival		Nivo-pluvial pre-alpine
Floodplain of national importance	La Sarine–Rossens-Fribourg (267 ha)		Senseauen (307 ha)

D_m: geometric mean; D_{90}: 90% finer.
[a]Classification according to Rinaldi *et al.* (2016).
[b]Source of the Cold Sense.

tributaries Gérine and Glâne with an annual average discharge of 1.7 and 4.2 $m^3\ s^{-1}$, respectively (Mapgeo, 2020; Figure 1). The discharge at the hydrological station 'Thörishaus–Sensematt' (located 20 km downstream of the Sense reach end; FOEN, 2020) is influenced by the Schwarzwasser as a main tributary (annual average discharge of 2.4 $m^3\ s^{-1}$; Mapgeo, 2020) located 3 km upstream of the station and two other smaller tributaries, the Laubbach and the Tütschbach (annual average discharge: ≤0.3 $m^3\ s^{-1}$; Mapgeo, 2020; Figure 1). It is most likely that, in the Sarine, floods with a return period of two (Q_2 = 260 $m^3\ s^{-1}$) or more years are not affected by hydropower operation (maximum capacity 99 $m^3\ s^{-1}$) and tributaries (e.g. Q_{200} Gérine = 140 $m^3\ s^{-1}$) located before the gauging station. Moreover, discharges ≥ Q_2 are expected to mobilize streambed sediments in both the Sarine and Sense reaches (Jaeggi, 2001; Jaeggi *et al.*, 2002; Ribeiro *et al.*, 2014).

The natural bedload transport downstream of the Rossens dam until the confluence with the tributary Gérine, located 1.4 km downstream of the hydropower plant Hauterive (Figure 1), was estimated by numerical model simulations at 4000 $m^3\ yr^{-1}$ (Jaeggi *et al.*, 2002), whereas the actual bedload transport is almost zero. The Gérine is estimated to transport

© 2020 John Wiley & Sons, Ltd.

Table 2. Historical evolution of residual flow released from the Rossens dam and maximum possible peak flow released from the hydropower plant Hauterive

Period	Residual flow (m^3 s^{-1})	Hydropeaking max. flow (m^3 s^{-1})
1948–1975	0.00	37.50
1976–1994	1.00	56.25
1994–2005	1.00	75.00
Since 2006	2.50–3.50	84.25[a]

Data source: personal communication Groupe-e (hydropower company).
[a]Maximum water volume that can pass through the turbines. However, only 75 m^3 s^{-1} can be legally released in the Sarine by the hydropower plant Hauterive.

3500 m^3 yr^{-1} in the Sarine (Jaeggi, 2001) and this volume has not changed significantly over the years. The bedload regime in the Sense reach is near-natural, with an estimated actual bedload supply from the Cold and Warm Sense of 7500 m^3 yr^{-1} (GEKOBE, 2014). However, an active period of mining occurred between 1950 and 2000 when important quantities of gravel were extracted from the Sense (1500–15 500 m^3 yr^{-1}). Additional information on the hydropower facilities, as well as on the flow and sediment regime, is provided in Supporting Information A.

Methods

Aerial images

Seven sets of historical aerial images and contemporary orthophotos captured over a period of 70–75 years were used to map and characterize morphological changes in the study reaches (Table 3). All images were obtained in digital format from the Swiss Federal Office of Topography (Swisstopo©). Images from 2007 and 2013 were SwissImage RGB orthophoto-mosaics at 25 cm resolution, and images from 1981 and 1993 were panchromatic orthophoto-mosaics at 50 cm resolution. Six time series of small- to medium-scale panchromatic vertical aerial images (Sarine: 1943, 1952, 1968; Sense: 1938, 1954, 1969) were obtained at scanning resolutions of 6.8–10.9 μm and then photogrammetrically processed, orthorectified and resampled to orthophoto-mosaics at 30 cm resolution (Supporting Information B).

Daily mean discharges at the date of the aerial surveys ranged between 2.3 and 10.8 m^3 s^{-1} in the Sense and between 10.9 and 88.7 m^3 s^{-1} in the Sarine (Table 3). According to the known residual flow regime (Table 2), except for 1943 (before damming), discharge in the Sarine-Residual is considered to be lower than 4 m^3 s^{-1}, whereas in the Sarine-Hydropeaking the recorded discharges are strongly affected by the hydropeaking regime.

Table 3. Characterization of the aerial images used and approximated daily mean discharge at the day of image acquisition.

Study reach	Flight date (dd.mm.yyyy)	# images used for final ortho-mosaic	Average flight height (m)	Focal length (mm)	Final pixel size (m)	Precision final ortho-mosaic (±m)	Daily mean discharge (m^3 s^{-1})
Sense							
	04.06.1938	2	3450	216.98-221.15	0.30	0.20†	9.9
	24.09 and 14.10.1954	2	4500-5000	210.1	0.30	0.34†	2.3–3.5
	14.07.1969	1	4500	152.87	0.30	0.25†	7.2
	01.06.1981	1	4762	153.02	0.50	nd	10.8
	29.07.1993	1	4819	152.52	0.50	nd	5.0
	01.08. and 21.09.2007 (ev.13.09)	1	2500–5000	nd	0.25	0.25‡	6.8 and 5.8 (ev.3.3)
	07.06.2013 (ev.31.07)	1	2500	nd	0.25	0.25‡	10.1 (ev.5.9)
Sarine-Residual and Sarine-Hydropeaking							
	30.08.1943	6	3000	204.08-212.77	0.30	0.13†	10.9
	08.04.1952	6	4300	210.38	0.30	0.71†	67.2
	25.06.1968	3	4200	152.87	0.30	0.37†	34.5
	01.06.1981	2	4306–4314	153.02	0.50	nd	66.0
	30.07.1993	1	5899	152.52	0.50	nd	45.2
	31.07.2007	1	2500	nd	0.25	0.25‡	48.4
	07.06.2013	1	2500	nd	0.25	0.25‡	88.7

nd: no data; ev: eventually.
†Average positional absolute accuracy (total image unit-weight RMSE).
‡Standard deviation for the precision in position.

© 2020 John Wiley & Sons, Ltd.

Habitat delimitation

The study area of each reach was delimited by the official perimeters of the floodplains of national importance 'La Sarine–Rossens-Fribourg' and 'Senseauen' (FOEN, 2007), with an additional buffer of 50 m to account for inaccuracies in the defined official perimeters. Upstream and downstream ends were delimited by the minor extent of the available aerial images (yellow polygons in Figure 1).

For each orthophoto-mosaic, six habitat types (i.e. geomorphic macro-units) were classified and manually digitized in ArcMap 10.4 (ESRI, Redlands, CA, USA) across the entire area of each reach (Table 4): (i) open water (OW); (ii) bare sediment (BS); (iii) vegetated sediment (VS); (iv) island (IS); (v) mature forest (MF); (vi) other structures (OS). Where necessary, digitized habitats were corrected for uncertainties (e.g. vegetation period, shaded areas) and digitalization artefacts (e.g. overlapping polygons, data gaps; Supporting Information C). Accuracy in habitat boundary delineation is commensurate with the final pixel resolution (0.25–0.5 m) and the final positional accuracy of the orthophoto-mosaics (max. ± 0.7 m; Table 3) as well as the possible digitization inaccuracy (estimated at ±2 m). These potential uncertainties were considered small relative to the expected amount of change between periods and the large-scale data provided by our study.

Floodplain and habitat variables, flood variables

Transformation of channel and floodplain morphology as well as physical habitats were quantified for the maximum active floodplain (MaxAF) area (orange polygons in Figure 1). We defined MaxAF as the union of OW, BS, VS and IS over the seven sets of digitized orthophoto-mosaics, thus representing the area where major morphological changes are expected due to flood activity of the last 70–75 years. For each reach,

Table 4. List and description of acronyms and variables employed in the text

	Habitat type
OW	Open water: primary and secondary lotic channels and standing waters
BS	Bare sediment: exposed cobble, gravel and sand surfaces free of vegetation cover
VS	Vegetated sediment: exposed cobble, gravel and sand surfaces with grass and/or pioneer vegetation such as different *Salix* sp. or *Petasites hybridus* as well as large woody debris
IS	Island: isolated dense vegetation growing on higher substrata and soil, surrounded either by OW, BS or VS, mainly colonized by *Alnus incana* and different *Salix* sp. but also hardwood vegetation. If there was a direct contact with MF, habitat class was MF
MF	Mature forest: dense vegetation fringing the active tract of the floodplain or outside of the floodplain, mainly colonized by *Alnus incana* and different *Fraxinus* sp. but also hardwood vegetation
OS	Other structures: including farming land (e.g. grassland, pasture, cultivated areas), hanging rock and cliffs free of vegetation cover, anthropogenic structures (e.g. buildings, industrial sites, reforestation zones)
Habitat unions	
AC	Active channel: union of OW and BS (e.g. Belletti *et al.*, 2014)
AF	Active floodplain: union of OW, BS, VS and IS
MaxAC	Maximum active channel: union of OW and BS over the seven sets of digitized orthophoto-mosaics (i.e. 70–75 years)
MaxAF	Maximum active floodplain: union of OW, BS, VS and IS over the seven sets of digitized orthophoto-mosaics (i.e. 70–75 years)
Floodplain and habitat variables	
Relative habitat proportion	Area proportion of each habitat type as percentage of the MaxAF area for each period between aerial images
AC width, AF width	AF and AC width for each period between aerial images, indicating narrowing/widening trends over time. Width was determined using automatically generated transect measurements evenly spaced (50 m) along and perpendicular to the centreline of the AF polygon and AC polygon, respectively
AC_{var}, AF_{var}	AC and AF median width variation (AC_{var} and AF_{var}, respectively; %), for each period between aerial images, normalized by the number of years between the consecutive periods (e.g. the percentage of AC_{var} between Sarine 1952 and Sarine 1968 rated by 16 years)
Habitat turnover rate	Number of changes in habitat types over the entire study period. First, vector data sets were converted into raster files of 2 m cell size with habitat classes coded by integer numbers. Then, all raster files of the same study reach were combined into a single raster file. This allowed the habitat type of each cell and year to be tracked and thus the habitat change of each cell through time to be computed
EA_{var}, VA_{var}	Eroded area variation EA_{var} (IS and/or MF and/or VS changed to AC, i.e. vegetation becoming AC; %) and vegetated area variation VA_{var} (AC changed to IS and/or MF and/or VS, i.e. AC becoming vegetation; %), for each period between aerial images, normalized by the number of years between the consecutive periods (e.g. Belletti *et al.*, 2014). Calculated from habitat turnover maps
VA/EA	Ratio between VA and EA for each period between aerial images, normalized by the number of years between the consecutive periods (e.g. Belletti *et al.*, 2014). VA/EA indicates the overall floodplain evolution (turnover) in terms of river and floodplain dynamics, including vegetation loss and gain and morphological erosion
SHDI, SHEI, MPS, MSI	Shannon's diversity index (SHDI), Shannon's evenness index (SHEI), mean shape size (MPS) and mean shape index (MSI) for each period between aerial images. Additional information is provided in Supporting Information F
Flood variables	
Q_2, Q_{10}, Q_{30}	Number of floods with return periods Q_2, Q_{10} and Q_{30}, normalized by the number of years between the consecutive periods. Each flood was considered only once (i.e. if one Q_{30} occurred, it was not also considered as Q_2 and Q_{10})
n.y. $Q \geq Q_2$	Maximum number of consecutive years with $Q \geq Q_2$, normalized by the number of years between the consecutive periods
n.m. $Q \geq Q_2$	Number of months since the most recent flood $Q \geq Q_2$
Q_{min}, Q_{max}, Q_{mean}, Q_{cv}	Flow minimum, maximum, mean and coefficient of variation

© 2020 John Wiley & Sons, Ltd.

we calculated a set of floodplain and habitat variables reflecting proportion, distribution, stability, diversity and patchiness (Table 4).

A set of flood variables that consider magnitude, frequency and timing of high-energy flood pulses and flow regime (Table 4), which could explain changes in channel and floodplain morphology as well as physical habitats, was calculated from maximum annual flow data of the selected hydrological stations (see 'Historical changes in flow and sediment regime', above) for the exact period between aerial image acquisition.

Statistical analyses

Spearman's correlations between single flood variables as control factors and floodplain/habitat variables (AC_{var}, AF_{var}, EA_{var}, VA_{var}, VA/EA) as response factors were used to analyse the dependence between flood activity and morphological changes. In addition, multiple linear regression (MLR) analyses were performed to test whether floodplain/habitat variables can be predicted by analysing a combination of different flood variables. Furthermore, to verify whether there is a reach effect, we fitted mixed-effect models (MEM) with the three different river reaches as block variables. Grouping the river reaches into three blocks, each with six samples (i.e. periods between aerial images), reduces the variability caused by the reach samples themselves and therefore leads to more accurate results (Bailey, 2008). To reduce multicollinearity in the MLRs and MEMs, two of the nine flood variables (Q_{max}, Q_{cv}) were excluded prior to model selection because of their significant Spearman's correlation ($p < 0.05$) with four other flood variables. Subsequently, the Akaike information criterion (AIC) was used to select the most appropriate model on a step-by-step basis with maximum likelihood estimates. After model selection, the MEMs were refitted with the restricted maximum likelihood method (REML) to obtain better variance estimates. Statistical analyses were performed using version 3.6.3 of the R software (R Development Core Team, 2008).

Results

Temporal changes in river flow regime and flood activity

During the pre-regulation period (1928–1943), before dam construction, the Sarine experienced the most flooding (Figures 2 and 4A and Table 5) with a flow mostly above the long-term daily mean (insert in Figure 2). The period 1943–1952 was influenced by construction of the dam (1944–1948) but still characterized by a similar amount of Q_2, Q_{10} and Q_{30} per year to that before flow regulation. The years 1952–1968 showed the same amount of Q_2 per year as the first two periods but no larger floods (Q_{10} and Q_{30}), whereas the years 1968–1981 showed a little less Q_2 but more Q_{10} per year than the three periods before. Subsequently, the number of Q_2 per year decreased. However, the major flood event occurred on 22 August 2005 with a magnitude of 750 $m^3\ s^{-1}$, corresponding to a Q_{115}. Moreover, the last three periods were characterized by no consecutive years with $Q \geq Q_2$. The period with the least flooding in the Sarine was the most recent (2007–2013), with one single Q_{30} at the beginning of the period and 70 months since the most recent flood $Q \geq Q_2$ (Table 5), as well as a flow over most of the period below the long-term daily mean. Furthermore, the mean maximum annual flow showed an important decrease from around 420–430 $m^3\ s^{-1}$ in the first two periods to 290–340 $m^3\ s^{-1}$ in the third and fourth period, 260 $m^3\ s^{-1}$ in the fifth and sixth period, and only 215 $m^3\ s^{-1}$ in the last period, corresponding to a reduction of approximately 50% compared to the first two periods and ~107 $m^3\ s^{-1}$ lower than the long-term mean maximum flow (Figure 2 and Table 5).

In the Sense, no clear decreasing trend in flooding frequency and magnitude was detectable (Figures 2 and 4A and Table 5). Most of the flooding occurred between 1954 and 1993, as well as between 2007 and 2013. The years 1938–1954 showed the least flooding, with only five Q_2 events in the 17-year period, no consecutive years with $Q \geq Q_2$, lowest mean maximum annual flow (~22 $m^3\ s^{-1}$ lower than the long-term mean maximum flow) and a flow mostly below the long-term daily mean (insert in Figure 2). The major flood event occurred on 29 July 1990 with a magnitude of 489 $m^3\ s^{-1}$, corresponding to a return period larger than 150 years.

Spatiotemporal changes in channel and floodplain morphology

From the pre-regulation period in 1943 to 2013, the proportion of BS area relative to the MaxAF area decreased by 52% in the Sarine-Residual and by 27% in the Sarine-Hydropeaking (Figure 3). Compared to 1943, original BS area decreased drastically by approximately 95% until 2013 in both hydropower-affected reaches. At the same time, the VS and MF areas increased by 95% and 319% in the Sarine-Residual, whereas in the Sarine-Hydropeaking VS decreased by 29% and MF increased by 149% (Figure 3).

In 1943 and 1952, the proportion of the active floodplain (AF) area of the Sarine-Residual was approximately 90% of the MaxAF area, which decreased by approximately 20% in 1968 and by an additional 18% in the last four periods (Figure 4B). At the same time, the proportion of the AC area relative to the maximum active channel (MaxAC) area decreased by approximately 44% until 1968 and then by a further 8% until 2013 (Figure 4C). The Sarine-Hydropeaking showed similar but less pronounced trends, with an AC and AF area decrease of approximately 25% between 1943 and 2013. The major flood event of 2005 (750 $m^3\ s^{-1} = Q_{115}$) coincided with a slight increase in AC and AF area but a decrease in BS and an increase in VS in 2007. Consistent with area changes, the residual and hydropeaking reaches underwent overall narrowing between the pre-regulation period (1943) and 2013, demonstrated by reductions in mean AC width of 62% and 33%, respectively (Figures 4E and 5; Supporting Information D). Similarly, mean AF width decreased by 42% and 29%, respectively (Figure 4D). Furthermore, although some differences in terms of habitat diversity and patchiness could be identified, there are no clear trends after dam construction (Supporting Information F).

In the near-natural Sense, between 1938 and 1954, the relative proportion of VS (+12%) and MF (+14%) area increased, whereas BS area decreased from 49% to 27%, although afterwards it varied between a minimum of 23% in 2013 and a maximum of 42% in 2007 (Figure 3). Interestingly, from 1954 until 2013, when the BS area increased, the VS area decreased almost proportionally, whereas its sum varied only slightly between 46% and 51% (Figure 3). Moreover, in 1938 the proportion of AC area relative to MaxAC area was 73% and the proportion of AF area in relation to MaxAF area was 83%; subsequently, they varied between 42% and 59% (Figure 4C) and between 58% and 68% (Figure 4B), respectively. Similarly, between 1938 and 1954 mean AC width and AF width

© 2020 John Wiley & Sons, Ltd.

decreased by 39% and 16%, respectively, but then they remained relatively stable with slight variation over the periods (Figure 4D,E; Supporting Information D). Surprisingly, the major flood event of 1990 (489 m^3 s^{-1}, $>Q_{150}$) coincided with a decrease in AC and AF area and width in the 1993 image.

In the study period lasting 70–75 years, 61% of the Sarine-Residual and 71% of the Sarine-Hydropeaking area, but only 34% of the Sense area, were characterized by either no changes or a maximum of two changes in habitat type, whereas 5–6% of the Sarine reaches area but 20% of the Sense area changed habitat type at least five times (Figure 6). Between 1943 and 2013, the Sarine-Residual underwent essential vegetation encroachment, seen by changes of 48% BS area and 89% VS area to MF and only 1% erosion of the vegetated areas VS and MF to BS (Supporting Information E). Moreover, 70% MF but only 3% BS and 2% VS area remained unchanged. Maximum vegetation encroachment in the Sarine-Residual occurred in the period 1952–1968, and conversely in the Sarine-Hydropeaking in the period 1981–1993. This is demonstrated by the approximately 25%

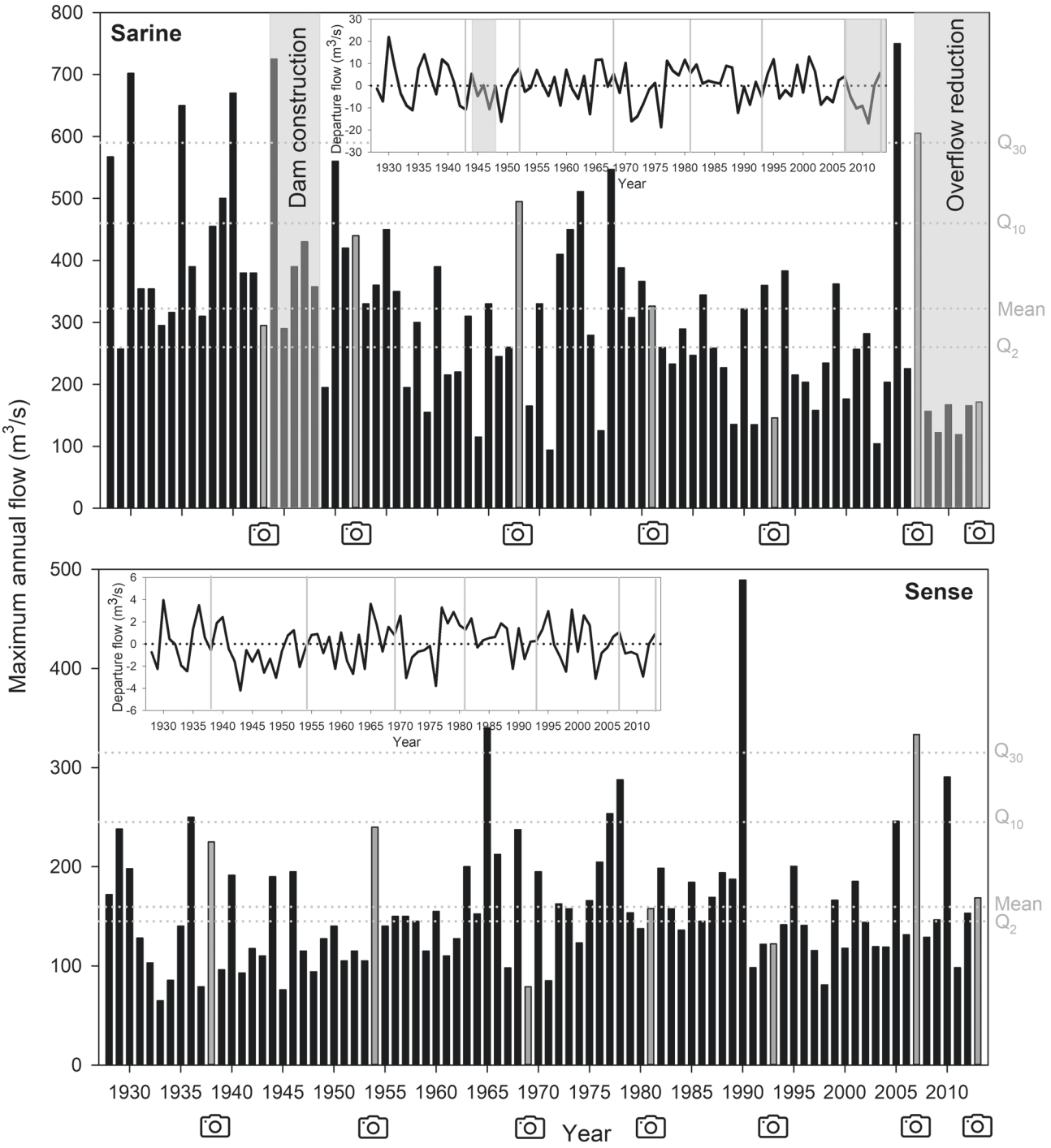

Figure 2. Histograms showing the maximum annual flow in the Sarine and in the Sense. Grey dotted lines indicate floods with return periods Q_2, Q_{10} and Q_{30} as well as the long-term mean maximum flow (1928–2013). Inset line plots show departure trends of annual mean daily flow series over the period of gauging. An ascending plot indicates periods that are persistently above mean flows; a descending plot indicates periods that are persistently below mean flows; and a level plot indicates flows near the long-term mean (dotted black line by zero). Camera icons and grey bars in the histogram plots and grey vertical lines in the line plots indicate the year of image acquisition (see Table 3 for exact dates). Grey squares indicate the construction period of the Rossens dam (1944–1948), and the period since the amount of dam overflow has been strongly reduced because of forecast software (since 2007). Note differenty-axis scales.

© 2020 John Wiley & Sons, Ltd.

Table 5. Flood variables calculated from maximum annual flow data for each period and study river (Sarine in black and Sense in grey colour). Q_2, Q_{10}, Q_{30} and n.y. $Q \geq Q_2$ are normalized by the number of years between consecutive periods. Each flood was considered only once (i.e. if one Q_{30} occurred, it was not also considered as Q_2 and Q_{10}). Flood variable acronyms are described in Table 4

	1928–43	1943–52	1952–68	1968–81	1981–93	1993–07	2007–13
Flood variable	1928–38	1938–54	1954–69	1969–81	1981–93	1993–07	2007–13
	0.63	0.63	0.63	0.54	0.42	0.21	0.00
Q_2	0.30	0.29	0.57	0.50	0.62	0.21	0.50
	0.13	0.13	0.00	0.23	0.00	0.00	0.00
Q_{10}	0.10	0.00	0.00	0.17	0.00	0.07	0.17
	0.19	0.13	0.00	0.00	0.00	0.07	0.14
Q_{30}	0.00	0.00	0.07	0.00	0.08	0.07	0.00
	0.88	0.63	0.31	0.31	0.00	0.00	0.00
n.y. $Q \geq Q_2$	0.30	0.00	0.29	0.42	0.46	0.00	0.33
	2	9	12	11	8	23	70
n.m. $Q \geq Q_2$	25	1	10	29	36	1	1
	257.00	195.00	115.00	94.00	135.09	104.18	118.89
Q_{min} ($m^3\ s^{-1}$)	64.80	76.00	98.00	79.00	98.12	80.87	98.13
	702.00	725.00	450.00	547.07	359.82	750.01	605.24
Q_{max} ($m^3\ s^{-1}$)	250.00	240.00	340.00	287.71	489.15	333.43	290.44
	429.69	420.94	291.56	343.76	261.44	264.23	215.33
Q_{mean} ($m^3\ s^{-1}$)	145.82	137.38	166.64	167.07	181.63	160.13	164.28
	33.79	38.63	33.32	42.67	28.09	60.38	80.47
Q_{cv}	45.50	36.80	38.13	36.91	53.63	40.60	40.38

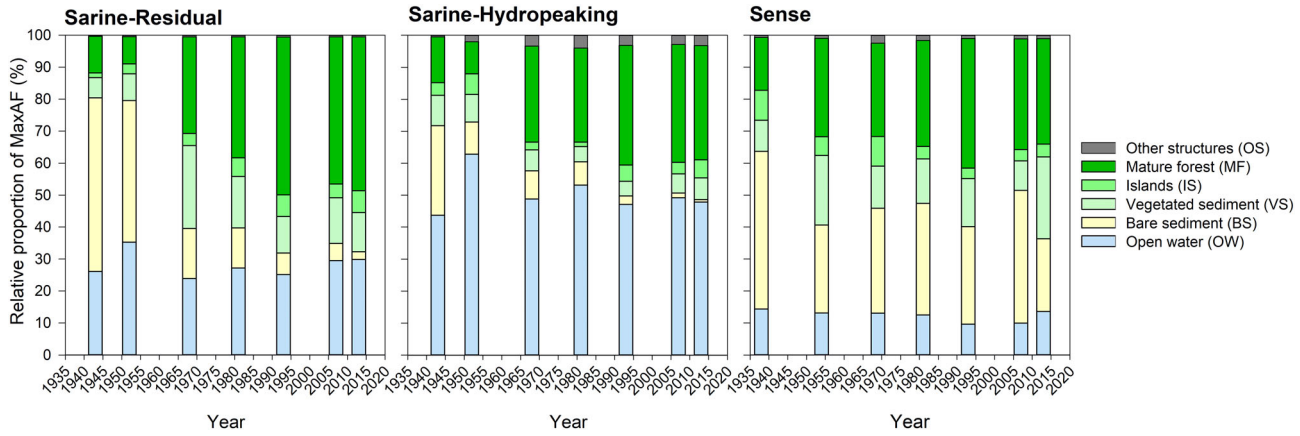

Figure 3. Area proportion of each habitat type expressed as percentage of maximum active floodplain area (MaxAF). See Table 3 for exact image acquisition dates.

of the BS area and 65% of the VS area that changed to MF in both reaches (Supporting Information E) and by the highest values of vegetated area variation in these periods (VA_{var}; i.e. AC becoming vegetation; Supporting Information D). In the Sense, between 1938 and 2013, 24% of the BS area and 46% of the VS area changed to MF, but in the same period also 19% of VS and 20% of MS areas changed to BS (Supporting Information E). Moreover, 51% MF, 23% BS and 20% VS area remained unchanged. Between 1938 and 1954, 16% of BS area, 49% of VS area and 58% of IS area changed to MF, whereas between 1993 and 2007 62% of the OW area, 55% of the VS area and 48% of the IS area changed to BS (Supporting Information E).

Relationship between flood activity and floodplain dynamics

Considering all three river reaches together, the variation of the active floodplain width (AF_{var}) was positively correlated to the flood variables Q_{30} and Q_{cv} (Table 6). In addition, 69% of the variation in AF_{var} can be predicted by the multiple linear regression (MLR) model with significant contribution of Q_{30} ($p < 0.001$) and, to a lesser extent ($p < 0.01$), also of Q_{10} and n.m. $Q \geq Q_2$ (i.e. number of months since the most recent flood $Q \geq Q_2$; Table 7). The variation of eroded areas (EA_{var}; i.e. vegetation becoming AC) was positively correlated with Q_{10} and to n.y. $Q \geq Q_2$ (i.e. maximum number of consecutive years with $Q \geq Q_2$; Table 6). More than 90% of the variation in EA_{var} can be explained by the MLR model, with significant contribution of Q_{30} and n.m. $Q \geq Q_2$ and to a lesser extent also of Q_{10} and n.y. $Q \geq Q_2$ (Table 7). In contrast, the variation of vegetated areas (VA_{var}; i.e. AC becoming vegetation) was negatively correlated with Q_{max} and Q_{mean}, and the MLR model explained 40% of the variation with significant contribution of Q_{mean} and Q_{min} (Tables 6 and 7). The AC width variation (AC_{var}) and the ratio of vegetated to eroded area (VA/EA) were not significantly correlated with any of the single flood variables (Table 6), and less than 35% of the variation in those variables can be explained by an MLR model.

© 2020 John Wiley & Sons, Ltd.

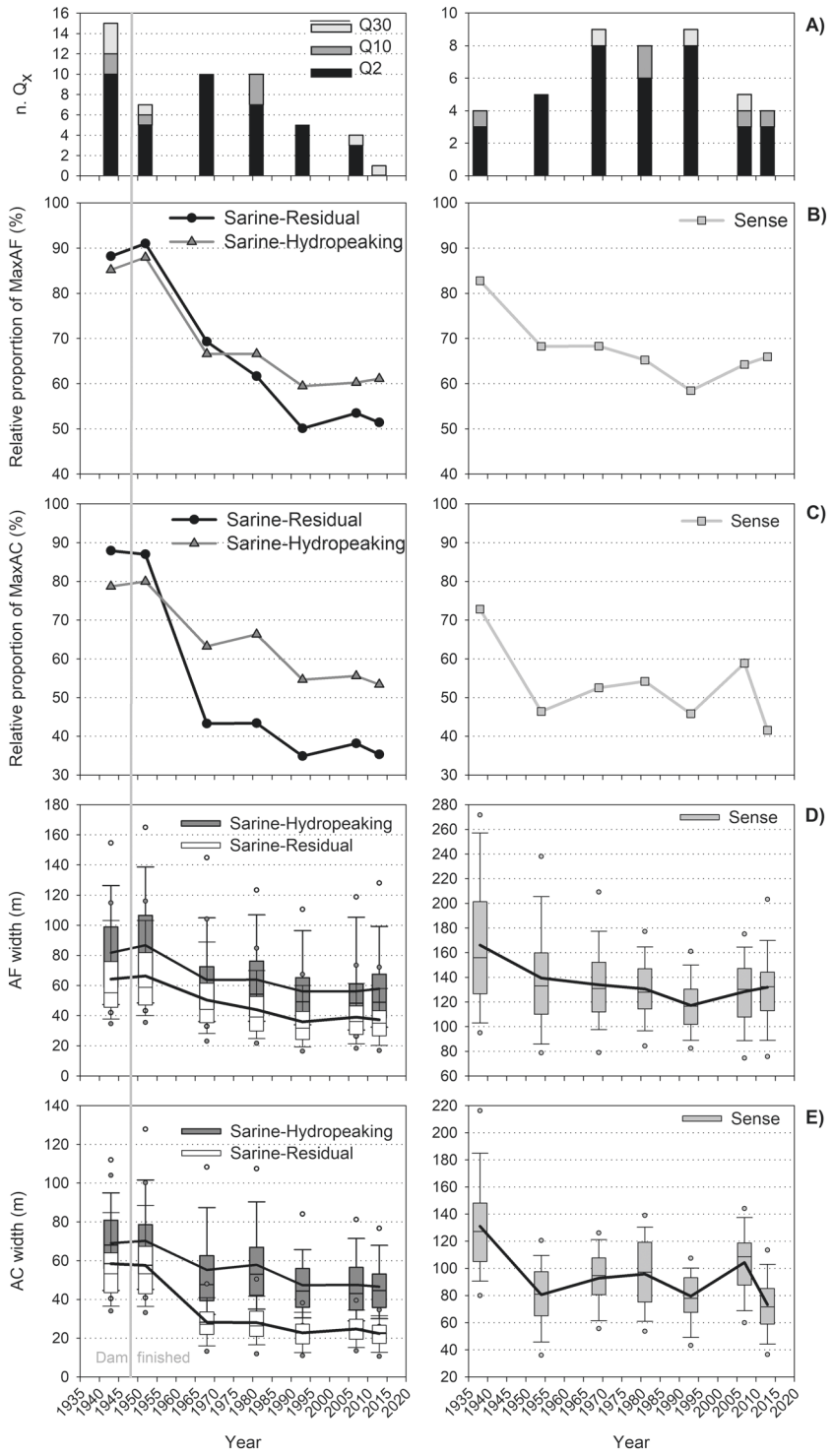

Figure 4. (A) Number of small ($Q_2 \leq Q < Q_{10}$), medium ($Q_{10} \leq Q < Q_{30}$) and large ($Q \geq Q_{30}$) floods for each period before the corresponding aerial image and for each study river (Sarine and Sense; see Table 3for exact image acquisition dates). (B) Proportion of active floodplain area (AF = OW + BS + VS + IS) expressed as percentage of maximum AF area (MaxAF) and (C) proportion of active channel area (AC = OW + BS) expressed as percentage of maximum AC area (MaxAC) for each study reach. (D) AF width and (E) AC width for each study reach. Boxplots in parts D and E show the 25th and 75thpercentiles, the median (black line in the box), whiskers (10th and 90th percentiles) and outliers (5th and 95th percentiles).The continuous thick black line connecting the boxes represents the mean. The grey solid vertical line indicates the date when the Rossens dam was finished (1948). Note different*y*-axis scales in parts A, D and E.

We could find no block effect for AC_{var} and AF_{var} as well as only a very slight, negligible block effect for EA_{var} and VA_{var} (i.e. no change in regard to significance of flood variables). Thus, for those four variables, there is no significant reach effect, meaning that all three river reaches react similarly to the flood variables. In contrast, VA/EA reacted differently to the flood variables in the Sarine-Hydropeaking compared with those in the Sarine-Residual and Sense (intercept values: −0.72, 0.54 and 0.18, respectively).

Discussion

Spatiotemporal changes in channel and floodplain morphology

Directional trends in morphological changes – relative habitat proportion, area and width of the AC and AF, turnover rate – were prominent and similar in the two hydropower-affected

© 2020 John Wiley & Sons, Ltd.

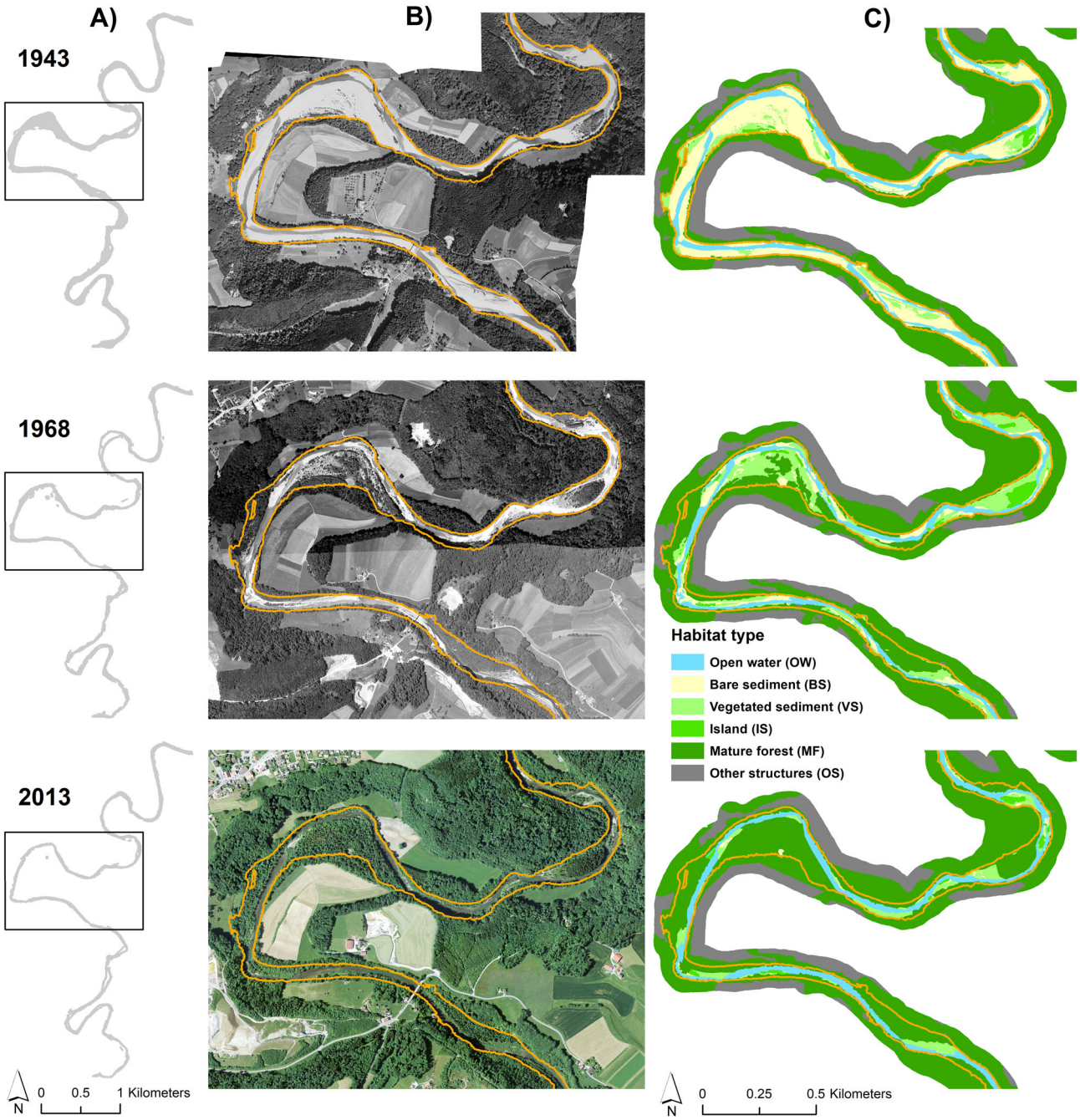

Figure 5. Example of morphological changes in the Sarine-Residual for the pre-regulation (1943) and two post-regulation periods (1968 and 2013). (A) Active channel area (AC = OW + BS) over the entire 11 km. The black polygons highlight the area presented in parts B and C. (B) Orthophotomosaics. (C) Habitat types. Orange polygons: maximum active floodplain area (MaxAF). Flow direction is from south to north.

reaches with, for example, original BS area drastically decreasing by up to 95% and vegetated areas (vegetated gravel bars, islands, mature forest) generally increasing from the pre-regulation period in 1943–2013, contrasting the lack of clear trends in the near-natural Sense (Figure 3). Doering *et al*. (2012) also found a decrease in BS area and an increase in vegetated areas within the first decades of water abstraction and levee impairment in the Urbach floodplain in Switzerland. However, changes were much less prominent, probably because in the Urbach only 30% of the annual baseflow is abstracted for hydropower production and flood events still occur on a regular basis.

In the Sarine, different periods of habitat and floodplain evolution could be distinguished with flood activity as the main driver. From the pre-regulation period (1943) until 4 years after dam completion (1952), flood activity remained almost constant (Figure 2 and Table 5) with no major habitat or floodplain changes (Figure 4). Between 1952 and 1968 the lack of medium–large floods (Q_{10}, Q_{30}) resulted in considerably decreasing area and narrowing of AC and AF, e.g. up to −44% in area and −51% for mean AC width in the Sarine-Residual (Figure 4), including vegetation encroachment (Supplementary Information D and E). Fairly constant habitat and floodplain evolution between 1968 and 1981 was then followed by further area and width reduction of AC and AF from 1981 to 1993 in conjunction with decreased flood occurrence until a new equilibrium was reached between 1993 and 2013 (Figure 4). These results are reflected in previous studies. For example, for 12 braided reaches of the Rhône basin (southeastern France), Belletti *et al*. (2014) observed a general AC narrowing during periods with no floods and widening after large floods over a period of approximately 50 years. Moreover, in a comprehensive review of morphological changes in Italian rivers over a period of 100 years, Surian and Rinaldi (2003)

© 2020 John Wiley & Sons, Ltd.

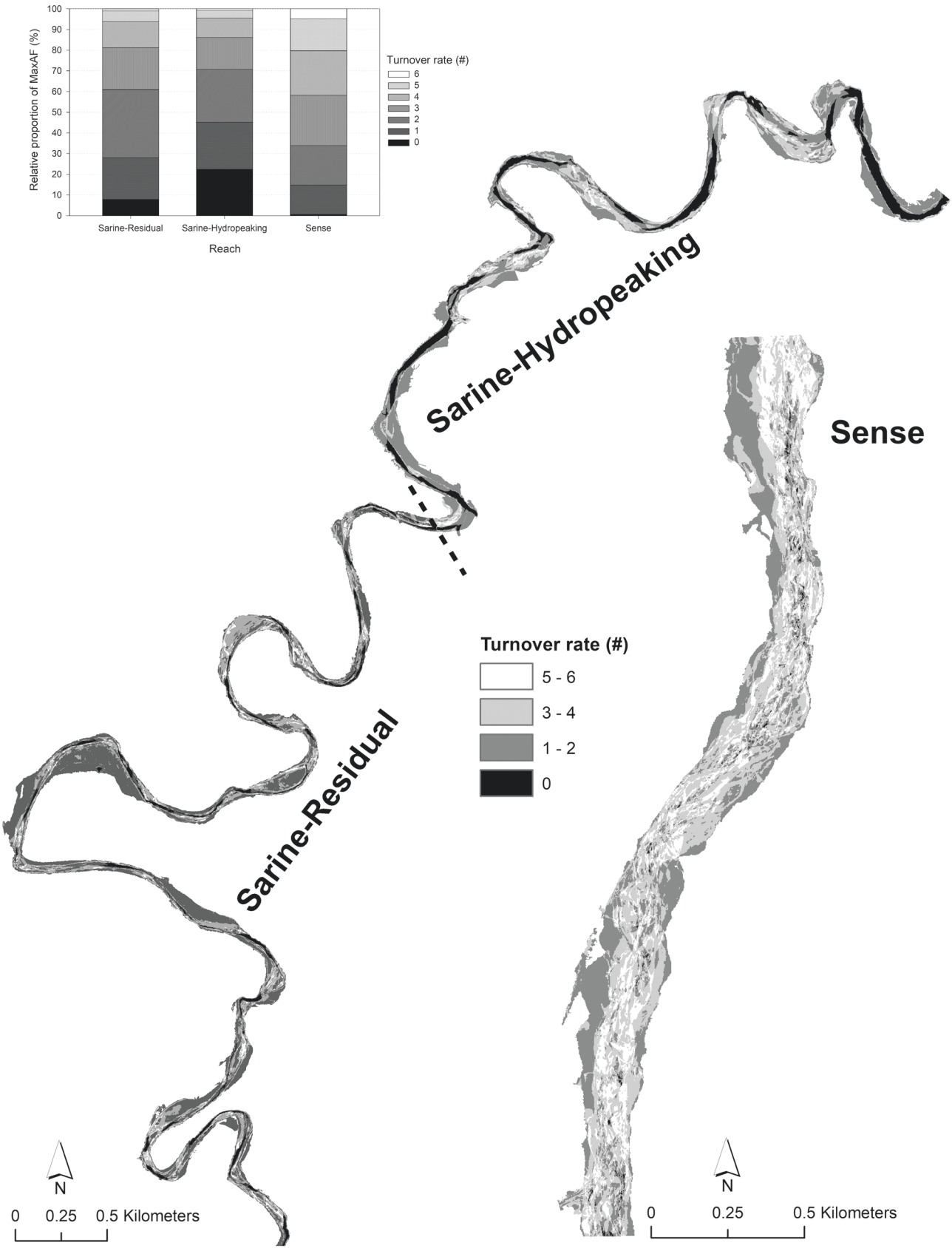

Figure 6. Spatial distribution of the number of changes (times per entire study period) in habitat types for the maximum active floodplain area (MaxAF) of the three study reaches from 1938/1943 to 2013. Black areas indicate no change in habitat type (turnover rate = 0), whereas brighter shades of grey indicate areas that shifted between different habitat types (turnover rates = 1–6). Dashed black line separates the Sarine residual and hydropeaking reaches. Flow direction is from south to north. The insert histogram plot shows the area proportion of each habitat turnover rate (0–6: number of changes in habitat types) over the entire study period expressed as percentage of MaxAF.

found channel narrowing up to 50% in response to various types of human disturbance such as dams, gravel mining and channelization. Further, similar to the 44% decrease in AC area of our study over a period of only 16 years (1952–1968), Garófano-Gómez *et al*. (2013) found a decrease in the pre-regulation AC area of approximately 80% 30–40 years after

© 2020 John Wiley & Sons, Ltd.

Table 6. Spearman's correlation coefficients between the floodplain/habitat and flood variables (acronyms are described in Table 4), for all three river reaches together ($n = 18$)

	Q_2	Q_{10}	Q_{30}	n.y. $Q \geq Q_2$	n.m. $Q \geq Q_2$	Q_{min}	Q_{max}	Q_{mean}	Q_{cv}
AC_{var}	−0.28	0.23	0.39	−0.21	0.17	−0.19	0.25	0.03	0.41
AF_{var}	−0.19	0.33	**0.55***	0.10	−0.07	0.05	0.35	0.01	**0.51***
EA_{var}	0.36	**0.62****	0.32	**0.59****	−0.15	−0.18	0.04	0.05	0.20
VA_{var}	0.16	−0.17	−0.31	0.13	−0.19	−0.24	**−0.71*****	**−0.58***	−0.39
VA/EA	−0.17	−0.45	−0.36	−0.29	0.00	0.05	−0.37	−0.33	−0.26

Significant correlations are indicated in bold, with $^*p < 0.05$, $^{**}p < 0.01$ and $^{***}p < 0.001$.

the beginning of hydropower flow regulation (decrease in flow magnitude and variability) in two alluvial reaches of the Mediterranean Mijares River (eastern Spain).

Notable habitat and floodplain changes in the near-natural Sense only occurred between 1938 and 1954 with decreasing BS area (−22%), and increasing vegetated areas (approximately +13%; Figure 3) as well as substantial area reduction and narrowing of AC and AF (e.g. up to −26% for the AC area and −39% for mean AC width) (Figure 4). These changes can most likely be attributed to sediment mining activities between 1950 and 2000 with maximum gravel extraction of approximately 15 000 m^3 yr^{-1} between 1970 and 1989 (Supporting Information A), as well as to levees installed for flood protection and bank stabilization in the 1950s (detected on the 1954 aerial images). Moreover, in the period 1938–1954 the Sense received a reduced number of morphologically effective floods (five Q_2 and no Q_{10} or Q_{30} in the 17-year period; Figures 2 and 4A and Table 5). Gostner *et al.* (2010) noted that bare sediment deposits in the Sense occur for $Q < Q_2$ but sediment deposits with pioneer vegetation (e.g. *Myricaria germanica*) are inundated at Q_2–Q_5; higher features such as islands with mature vegetation at $Q > Q_5$, and all parafluvial features are inundated when discharges exceed a 20-year return period. After 1954, the Sense AF experienced recurrent narrowing and widening as well as changes between bare and vegetated areas, with no directional trend (Figures 3 and 4), which was most probably caused by similar flood conditions between 1954 and 2013 (Figure 2 and Table 5). However, the major flood event of 1990 (489 m^3 s^{-1}, $> Q_{150}$) coincided with an increase in vegetated area. Two dry years (1991 and 1992), the lack of Q_{10} between 1981 and 1993 and the absence of floods $\geq Q_2$ for 36 months (Figure 2 and Table 5), as well as the short duration of the major flood event (the daily mean flow on 29 July 1990 was 34.6 m^3 s^{-1}) might explain vegetation encroachment and stabilization and thus this unexpected behaviour.

Table 7. Best (Akaike information criterion) multiple linear regression (MLR) model for prediction of the floodplain/habitat variables by a combination of flood variables (acronyms are described in Table 4), for all three river reaches together ($n = 18$). For VA/EA, results of the REML model are reported because of significant block effect

	Adjusted R^2	Estimate (β) and p-values
AC_{var}	0.29	Intercept: −4.83 **Q_2: 15.39*** **Q_{10}: 16.09*** **Q_{30}: 53.80**** **n.y. $Q \geq Q_2$: −15.47*** Q_{min}: −0.02
AF_{var}	0.69	Intercept: 0.20 Q_2: −1.32 **Q_{10}: 5.87**** **Q_{30}: 15.95***** **n.m. $Q \geq Q_2$: −0.03**** Q_{mean}: −0.00
EA_{var}	0.92	Intercept: 0.45 **Q_{10}: 6.05**** **Q_{30}: 19.54***** **n.y. $Q \geq Q_2$: 2.40**** **n.m. $Q \geq Q_2$: −0.04***** Q_{mean}: −0.00 Q_{min}: 0.01
VA_{var}	0.40	**Intercept: 3.02**** Q_{10}: 6.83 Q_{30}: −10.05 **Q_{mean}: −0.02**** **Q_{min}: 0.04*** Intercept: 1.14
VA/EA	0.34	**Q_{10}: −8.98*** **Q_{30}: −27.21**** n.m. $Q \geq Q_2$: 0.03 Q_{min}: 0.02

Estimate of regression beta coefficients and significant t-statistic p-values are indicated in bold, with $^*p < 0.05$, $^{**}p < 0.01$ and $^{***}p < 0.001$.

In the two hydropower-affected reaches of the Sarine, turnover rate over the 70-year study period (1943–2013; seven observations) was low, with approximately only 5% of the total floodplain area analysed changing habitat type five to six times. This coincides with turnover rates in the Urbach floodplain (Switzerland), impacted by water abstraction and levees, where only 5% of the floodplain changed habitats at least four times in the 67-year study period (1940–2007; seven observations; Doering *et al.*, 2012). In contrast, floodplain turnover in the near-natural Sense over the 75-year study period (1938–2013; seven observations) was frequent, where 20% of the floodplain area changed habitat type five to six times and less than 1% remained unchanged (Figure 6). This corresponds to turnover rates found in the natural Nyack floodplain in north-western Montana (USA), where 25% of the floodplain changed habitats at least four times in the 59-year study period (1945–2004; nine observations; Whited *et al.*, 2007). Despite the frequent habitat change in the Nyack and Sense (after 1954), the relative proportion of the habitat types remained relatively constant, supporting the shifting habitat mosaic concept (Stanford *et al.*, 2005) typical of natural floodplains.

The different valley confinement and floodplain planform of the Sarine (partly confined, single-thread meandering, actual channel slope 2–3‰) and Sense (laterally unconfined, multi-thread braided river, actual channel slope 17‰) reaches can partly explain the different floodplain changes. However, the main drivers of the morphological changes in the Sarine reaches described above are most likely linked to the drastically reduced flood activity (Figure 2 and Table 5) and truncation of bedload and suspended sediment supply downstream of the dam. The resulting shift from a depositional (pre-regulation) to an erosional (post-regulation) state is most likely associated with vegetation-driven stabilization processes and vegetation encroachment promoted by the 70 years of hydropower exploitation. According to Jaeggi *et al.* (2002), in the depositional state the Sarine could move over the entire AC and AF, whereas in the erosional state, in particular under residual flow conditions, flow

© 2020 John Wiley & Sons, Ltd.

is mainly limited to the main channel and connections with secondary branches have almost disappeared; and, further, the lack of incoming bedload promoted incision of the river. During the erosional state, vegetation may find favourable conditions to develop, the recruitment being maximized and the scouring minimized. Moreover, vegetation patches and plants roots stabilize sediments and banks and reduce lateral erosion, favouring bed stability and channel straightening, thereby also reducing habitat turnover by high-energy floods (Gurnell *et al.*, 2012; Camporeale *et al.*, 2013; Gurnell, 2014; and references therein). In the Sarine, floodplain narrowing as well as vegetation development and stabilization moved from upstream to downstream over time. For example, major vegetation encroachment in the hydropeaking reach, located 13 km downstream of the dam, occurred approximately 30 years later than in the residual reach (Supporting Information D and E). Moreover, the tributary Gérine carries 3500 m^3 sediment per year into the Sarine (Jaeggi, 2001), which may prolongate reaction time for channel incision and floodplain disconnection including mature vegetation development and bed stabilization.

Interaction between flood activity and floodplain dynamic

We found that channel and floodplain morphology as well as physical habitats dynamic are, in large part, dependent on flood series characters. Indeed, for the three river reaches investigated, we were able to show that active floodplain widening (AF_{var}) and erosion of vegetated areas (EA_{var}) most likely prevail during periods with medium–large floods (Q_{10}, Q_{30}) in conjunction with consecutive floods $Q \geq Q_2$ (Tables 6 and 7). The magnitude and frequency of these high-energy flood pulses are assumed to limit vegetation establishment on bare gravel bars within the bankfull boundaries (parafluvial). Further, discharges $\geq Q_2$ are expected to mobilize streambed sediments in the Sarine (Jaeggi, 2001; Jaeggi *et al.*, 2002; Ribeiro *et al.*, 2014). However, even the two high-magnitude flooding events of 2005 (750 $m^3\ s^{-1} = Q_{115}$) and 2007 (605 $m^3\ s^{-1} = Q_{34}$) had almost no morphological effect on the Sarine reaches. This suggests that stabilization by vegetation encroachment in the Sarine restricts lateral erosion even under large flood conditions, limiting floodplain responses to flood events. Similarly, Belletti *et al.* (2014, 2015) found that floodplain patterns in general and AC width in particular are primarily controlled by Q_{10} floods, but not all reaches respond systematically to each Q_{10} flood. Discontinuous floodplain response to changing flow and sediment regimes is probably a result of the hydrogeomorphological variability and dynamic nature of floodplains varying in temporal and spatial scales within the geographic, human and climatic context (Welber *et al.*, 2012; Belletti *et al.*, 2014; Toone *et al.*, 2014; Church and Ferguson, 2015; Wohl *et al.*, 2015a); thus trend generalization is extremely difficult based solely on flood magnitude and duration. Nevertheless, according to Belletti *et al.* (2014), we conclude that medium- to large-energy floods with return periods higher or equal to 10 years (e.g. Q_{10}, Q_{30}) act as important drivers for spatiotemporal floodplain reorganization and dynamics. Further, 10–30 years is most likely a timescale during which essential floodplain narrowing and changes in habitat proportion and distribution can be expected after the beginning of flow and sediment regulation by hydropower installations. However, the effects of flow regulation on vegetation structure are, in many cases, still not complete after many decades (Nilsson and Svedmark, 2002; González *et al.*, 2010; Garófano-Gómez *et al.*, 2013) or even centuries (Johnson, 1992).

Conclusion and Implications for Restoration Actions

The analysis of two hydropower-affected reaches and one near-natural reach located in protected floodplains of the Swiss pre-Alps between 1938/1943 and 2013 supports our initial expectation of an existing relationship between the modification of the natural flow and sediment regime and the transformation of channel and floodplain morphology and dynamics. However, this relationship is spatiotemporally complex. For instance, the results of our study indicate major and faster impacts in the Sarine residual flow reach, which is located directly downstream of the hydropower dam and lacks sediment delivery from tributaries, with a dramatic reduction of BS area, AC and AF areas, important narrowing and very low habitat turnover rates, indicating vegetation encroachment. In contrast, after an initial period of sediment mining activities and reduced high-energy flood events, the near-natural Sense exhibited recurrent narrowing and widening, and changes between bare and vegetated areas with no clear directional trend over time, as well as frequent habitat turnover rates. Moreover, our results suggest that floodplain evolution and dynamics follow a complex trajectory related to magnitude, frequency and timing of floods, as well as sediment availability and vegetation dynamics. Medium–large floods (Q_{10}, Q_{30}) in combination with consecutive floods $Q \geq Q_2$ generally support AF widening and erosion of vegetated areas, whereas periods of low flooding frequency favour morphological stability as a result of vegetation succession. However, also extremely high-energy flood events (e.g. $> Q_{150}$ in the Sarine), if of short duration and in-between periods with relatively low flow and flood conditions, do not necessarily imply relevant morphological effects in these floodplains. Furthermore, we were able to highlight that radical changes already appear only a few decades (e.g. approximately 20 years in the Sarine residual flow reach) after alteration of the natural flow and sediment regime until a new equilibrium is reached. Finally, based on the floodplain/habitat variables used in this study, changes in active floodplain width (AF_{var}) and in eroded areas (EAvar; i.e. vegetation becoming AC) are best suited for assessing morphological effects of flood variables in complex floodplains. Overall, consideration of these quantitative results and application of appropriate variables to the hydrogeomorphological evolution of the hydropower-regulated river floodplain of the Sarine could serve as a framework for restoration activities in general.

Dam removal, a measure which is increasingly being considered for hydromorphological river restoration (e.g. Ritchie *et al.*, 2018), is almost certainly socioeconomically unacceptable for the longest and fourth largest Swiss reservoir and its importance for energy production and flexibility, in particular in the context of the staggered withdrawal from nuclear energy in Switzerland (SFOE, 2020). Valuable alternatives are controlled artificial floods, a well-accepted restoration measure in river systems affected by dams (Konrad *et al.*, 2011; Robinson, 2012; Olden *et al.*, 2014; Wohl *et al.*, 2015b). An artificial flood with a maximum magnitude of 195 $m^3\ s^{-1}$ (~100× the actual residual flow and corresponding approximately to a Q_2) was released from the Rossens dam in the Sarine in September 2016. Before flooding, sediment deposits were added to the river downstream of the dam, and mature vegetation was locally removed from the banks and bars to promote lateral erosion and to prevent further channel incision and floodplain disconnection. This combination of measures successfully increased morphological diversity and related hydraulic habitat suitability (Stähly *et al.*, 2019), habitat turnover, local removal of pioneer vegetation on sediments

© 2020 John Wiley & Sons, Ltd.

deposits and also partial inundation of higher features such as islands and alluvial forest (Doering *et al.*, 2018). However, effects were only short term, in particular for aquatic macroinvertebrates, algal growth and pioneer vegetation (Doering *et al.*, 2018), suggesting a regular implementation of floods of varying size and timing for sustainable management and long-term effect on ecosystem structure and function (*sensu* Palmer and Ruhi, 2019). This has been demonstrated, for instance, in a long-term study on the release of artificial floods in the Swiss River Spöl (Robinson, 2012; Robinson *et al.*, 2018).

The results from our historical analyses can serve as an important baseline for the design of a long-term environmental flow program, including experimental flooding in the Sarine and eventually also in other floodplain rivers of the Alps. This suggests the implementation of elements of the historical, pre-dam flow regime, with consecutive years of low-magnitude floods (e.g. Q_2), in combination with some medium–large floods (e.g. Q_{10}, Q_{30}) every 10–30 years. Further, sediment replenishments and vegetation clearance would probably favour lateral reactivation and erosion of vegetated areas and sediment aggradation, which would ultimately lead to AC widening and overall reactivation of the entire Sarine floodplain. However, implementing a long-term environmental flow program needs a rigorous and concomitant adaptive management process involving authorities, hydropower plant owners, specialized consulting firms, scientists and other appropriate stakeholders. Adaptive management is mandatory to determine, monitor and adapt, if necessary, measures such as the amount of sediment replenishment, flood magnitude and frequency or vegetation clearance, as well as to balance ecomorphological and socioeconomic (e.g. water for electricity production, flood protection) needs. Finally, it should be considered that, after the implementation of restoration measures, the timescale for large-scale channel and floodplain evolution is probably medium to long (30–80 years).

Acknowledgements

This project was supported by the Swiss National Science Foundation (SNSF, Project No. 407040_153972) as part of the National Research Program 70 'Energy Turnaround' (NRP 70, www.nrp70.ch). The authors are especially grateful to S. Friedli and F. Rickenbacher, who performed habitat digitalization of the orthophoto-mosaics. We thank two anonymous reviewers for helpful comments, which greatly improved the manuscript. All authors have no conflicts of interest to declare.

Data Availability Statement

The data sets used and/or analysed during the current study are available from the corresponding author on reasonable request.

References

Bailey RA. (2008) Blocking. In Bailey RA (ed.) *Design of Comparative Experiments*. Cambridge Series in Statistical and Probabilistic Mathematics. Cambridge University Press, Cambridge, UK, pp. 53–74.

Belletti B, Dufour S, Piégay H. 2014. Regional assessment of multi-decadal changes in braided riverscapes following large floods (example of 12 reaches in south east of France). *Advances in Geosciences* **37**: 57–71.

Belletti B, Dufour S, Piégay H. 2015. What is the relative effect of space and time to explain the braided river width and island patterns at a regional scale? *River Research and Applications* **31**: 1–15.

Belletti B, Rinaldi M, Bussettini M, Comiti F, Gurnell AM, Mao L, Nardi L, Vezza P. 2017. Characterising physical habitats and fluvial hydromorphology: a new system for the survey and classification of river geomorphic units. *Geomorphology* **283**: 143–157.

Best J. 2019. Anthropogenic stresses on the world's big rivers. *Nature Geoscience* **12**: 7–21.

Braillard L, Mauvilly M. 2008. Morphogenesis of the Sarine canyon in the Plateau Molasse, Switzerland: new data from an archaeological site. *Geographica Helvetica* **63**: 181–187.

Bunn SE, Arthington AH. 2002. Basic principles and ecological consequences of altered flow regimes for aquatic biodiversity. *Environmental Management* **30**: 492–507.

Camporeale C, Perucca E, Ridolfi L, Gurnell AM. 2013. Modeling the interactions between river morphodynamics and riparian vegetation. *Reviews of Geophysics* **51**: 379–414.

Church M, Ferguson RI. 2015. Morphodynamics: rivers beyond steady state. *Water Resources Research* **51**: 1883–1897.

Doering M, Blaurock M, Robinson CT. 2012. Landscape transformation of Alpine floodplain influenced by humans: historical analyses from aerial images. *Hydrological Processes* **26**: 3319–3326.

Doering M, Tonolla D, Robinson CT, Schleiss A, Stähly S, Gufler C, Geilhausen M, Di Cugno N. 2018. Künstliches Hochwasser an der Saane: Eine Massnahme zum nachhaltigen Auenmanagement. [Artificial flooding in the Saane: a measure for sustainable floodplain management]. *Wasser Energie Luft* **2**: 119–127.

FOEN. (2007) *Inventory of floodplain of national importance*. Federal Office for the Environment, Ittigen, Switzerland. Available: http://www.bafu.admin.ch/auen [15 October 2020].

FOEN. (2020). Hydrological data. Federal Office for the Environment, Ittigen, Switzerland. Available: https://www.hydrodaten.admin.ch/en/ [19 July 2020].

Garófano-Gómez V, Martìnez-Capel F, Bertoldi W, Gurnell A, Estornell J, Segura-Beltrán F. 2013. Six decades of changes in the riparian corridor of a Mediterranean river: a synthetic analysis based of historical data source. *Ecohydrology* **6**: 536–553.

GEKOBE. (2014). Gewässerentwicklungskonzept Bern. Strategische Planungen nach GSchG/GSchV: Sanierung des Geschiebehaushaltes im Kanton. Schlussbericht: Gewässersystem Sense–Saane–Aare. [Berne river development concept. Strategic planning according to WPA/WPO: mitigation of the bedload budget in the canton. Final report: Sense–Saane–Aare river system]. Bau-, Verkehrs- und Energiedirektion (BVE), Canton Bern; 19

Gigot H. 1950. Le Barrage de Rossens. [The Rossens dam]. In *Nouvelles étrennes fribourgeoises*. Fragnière Frères: Fribourg; 16.

González E, González-Sanchis M, Cabezas Á, Comín F, Muller E. 2010. Recent changes in the riparian forest of a large regulated Mediterranean river: implications for management. *Environmental Management* **45**: 669–681.

Gostner W, Schleiss AJ, Annable WK, Paternolli M. 2010. Gravel bar inundation frequency: an indicator for the ecological potential of a river. In *Proceedings of River Flow 2010 Conference*, Dittrich A, Aberle J, Geisenhainer P (eds). Bundesanstalt für Wasserbau: Braunschweig; 1485–1493.

Grabowski RC, Surian N, Gurnell AM. 2014. Characterizing geomorphological change to support sustainable river restoration and management. *WIREs Water* **1**: 483–512.

Graf WL. 2006. Downstream hydrologic and geomorphic effects of large dams on American rivers. *Geomorphology* **79**: 336–360.

Grill G, Lehner B, Thieme M, Geenen B, Tickner D, Antonelli F, Babu S, Borrelli P, Cheng L, Crochetiere H, Macedo HE. 2019. Mapping the world's free-flowing rivers. *Nature* **569**: 215–221.

Gurnell AM. 2014. Plants as river system engineers. *Earth Surface Processes and Landforms* **39**: 4–25.

Gurnell AM, Bertoldi W, Corenblit D. 2012. Changing river channels: the roles of hydrological processes, plants and pioneer fluvial landforms in humid temperate, mixed load, gravel bed rivers. *Earth-Science Reviews* **111**: 129–141.

Hettrich R, Ruff A, Tranter C, Rast G, Köberich T. 2011. *Freiheit für das wilde Wasser. Status und Perspektiven nordalpiner Wildflusslandschaften aus naturschutzfachlicher Sicht. [Freedom for*

© 2020 John Wiley & Sons, Ltd.

Wild Waters: Status and Perspectives of Northern Alpine Wild River Landscapes from a Nature Conservation Perspective]. WWF: Berlin.

Hohensinner S, Jungwirth M, Muhar S, Schmutz S. 2011. Spatio-temporal habitat dynamics in a changing Danube river landscape 1812–2016. *River Research and Applications* **27**: 939–955.

IEA. (2018) *Key World Energy Statistics (2016 data)*. International Energy Agency: Paris. Available: https://webstore.iea.org/key-world-energy-statistics-2018 [15 October 2020].

Jaeggi M. 2001. Charriage de la Sarine entre la Gérine et le Lac de Pérolles. [Bedload of the Sarine between the Gérine and the Lake of Pérolles]. Rapport technique; 13.

Jaeggi M, Hunziker R and Ryser A. 2002 Petite-Sarine. Etude sur l'incidence du barrage de Rossens sur la morphologie fluviale, le charriage et l'évolution future de cette zone alluviale. [Little-Sarine. Study on the impact of the Rossens dam on the river morphology, the bedload and the future evolution of this alluvial zone]. Rapport technique; 29.

Johnson WC. 1992. Dams and riparian forests: case study from the Upper Missouri River. *Rivers* **3**: 229–242.

Konrad CP, Olden JD, Lytle DA, Melis TS, Schmidt JC, Bray EN, Freeman MC, Gido KB, Hemphill NP, Kennard MJ, McMullen LE. 2011. Large-scale flow experiments for managing river systems. *Bioscience* **61**: 948–959.

Lallias-Tacon S, Liébault F, Piégay H. 2017. Use of airborne LiDAR and historical aerial photos for characterising the history of braided river floodplain morphology and vegetation responses. *Catena* **149**: 742–759.

Mapgeo. 2020. Mapping platform of the Swiss Confederation. Available: https://map.geo.admin.ch/ [15 October 2020].

Meile T, Boillat JL, Schleiss A. 2011. Hydropeaking indicators for characterization of the Upper-Rhone River in Switzerland. *Aquatic Sciences* **73**: 171–182.

MeteoSwiss. 2017. Precipitation data. Federal Office of Meteorology and Climatology, Zurich, Switzerland. Available: http://www.meteoswiss.admin.ch [15 October 2020].

Moog O. 1993. Quantification of daily peak hydropower effects on aquatic fauna and management to minimize environmental impacts. *Regulated Rivers: Research and Management* **8**: 5–14.

Nilsson C, Svedmark M. 2002. Basic principles and ecological consequences of changing water regimes: riparian plant communities. *Environmental Management* **30**: 468–480.

Olden JD, Konrad CP, Melis TS, Kennard MJ, Freeman MC, Mims MC, Bray EN, Gido KB, Hemphill NP, Lytle DA, McMullen LE. 2014. Are large-scale flow experiments informing the science and management of freshwater ecosystems? *Frontiers in Ecology and the Environment* **12**: 176–185.

Palmer M, Ruhi A. 2019. Linkages between flow regime, biota, and ecosystem processes: implications for river restoration. *Science* **365**: eaaw2087. https://doi.org/10.1126/science.aaw2087

Poff NL, Allan JD, Bain MB, Karr JR, Prestegaard KL, Richter BD, Sparks RE, Stromberg JC. 1997. The natural flow regime: a paradigm for river conservation and restoration. *Bioscience* **47**: 769–784.

Poff NL, Olden JD, Merritt DM, Pepin DM. 2007. Homogenization of regional river dynamics by dams and global biodiversity implications. *Proceedings of the National Academy of Sciences USA* **104**: 5732–5737.

Poff NL, Zimmermann JKH. 2010. Ecological responses to altered flow regimes: a literature review to inform the science and management of environmental flows. *Freshwater Biology* **55**: 194–205.

R Development Core Team. (2008). R: A Language and environment for statistical computing. Available: https://www.r-project.org [15 October 2020].

Ribeiro ML, Wampfler S, Schleiss AJ. 2014. Morphodynamic changes in a natural river confluence due to a hydropower modified flow regime. In *Swiss Competence in River Engineering and Restoration*, Schleiss AJ, Speerli J, Pfamatter R (eds). Taylor & Francis: London; 191–199.

Richter BD, Mathews R, Harrison DL, Wigington R. 2003. Ecologically sustainable water management: managing river flows for ecological integrity. *Ecological Applications* **13**: 206–224.

Rinaldi M, Gurnell AM, González del Tánago M, Bussettini M, Hendriks M. 2016. Classification of river morphology and hydrology to support management and restoration. *Aquatic Sciences* **8**: 17–33.

Ritchie AC, Warrick JA, East AE, Magirl CS, Stevens AW, Bountry JA, Randle TJ, Curran CA, Hilldale RC, Duda JJ, Gelfenbaum GR. 2018. Morphodynamic evolution following sediment release from the world's largest dam removal. *Scientific Reports* **8**: 13279. https://doi.org/10.1038/s41598-018-30817-8

Robinson CT. 2012. Long term changes in community assembly, resistance and resilience following experimental floods. *Ecological Applications* **22**: 1949–1961.

Robinson CT, Siebers AR, Ortlepp J. 2018. Long-term ecological responses of the River Spöl to experimental floods. *Freshwater Science* **37**: 433–447.

SFOE. 2019. *Stand der Wasserkraftnutzung in der Schweiz am 31. Dezember 2019. [Status of Hydropower Use in Switzerland on December 31 2019]*. Swiss Federal Office of Energy: Ittigen, Switzerland.

SFOE. (2020). Energy strategy 2050. Swiss Federal Office of Energy, Ittigen, Switzerland. Available at: https://www.bfe.admin.ch/bfe/en/home/policy/energy-strategy-2050.html

Stähly S, Franca MJ, Robinson CT, Schleiss AJ. 2019. Sediment replenishment combined with an artificial flood improves river habitats downstream of a dam. *Scientific Reports* **9**: 5176. https://doi.org/10.1038/s41598-019-41575-6

Stanford JA, Lorang MS, Hauer FR. 2005. The shifting habitat mosaic of river ecosystems. *Verhandlungen: Internationale Vereinigung fur Theoretische und Angewandte Limnologie* **29**: 123–136.

Surian N, Rinaldi M. 2003. Morphological response to river engineering and management in alluvial channels in Italy. *Geomorphology* **50**: 307–326.

Tockner K, Lorang MS, Stanford JA. 2010a. River flood plains are model ecosystems to test general hydrogeomorphic and ecological concepts. *River Research and Applications* **26**: 76–86.

Tockner K, Pusch M, Borchardt D, Lorang MS. 2010b. Multiple stressors in coupled river–floodplain ecosystems. *Freshwater Biology* **53**: 135–151.

Tockner K, Stanford JA. 2002. Riverine flood plains: present state and future trends. *Environmental Conservation* **29**: 308–330.

Toone J, Rice SP, Piégay H. 2014. Spatial discontinuity and temporal evolution of channel morphology along a mixed bedrock–alluvial river, upper Drôme River, southeast France: contingent response to external and internal controls. *Geomorphology* **205**: 5–16.

Vörösmarty CJ, McIntyre PB, Gessner MO, Dudgeon D, Prusevich A, Green P, Glidden S, Bunn SE, Sullivan CA, Liermann CR, Davies PM. 2010. Global threats to human water security and river biodiversity. *Nature* **467**: 555–561.

Ward JV, Tockner K, Arscott DB, Claret C. 2002. Riverine landscape diversity. *Freshwater Biology* **47**: 517–539.

Welber M, Bertoldi W, Tubino M. 2012. The response of braided planform configuration to flow variations, bed reworking and vegetation: the case of the Tagliamento River, Italy. *Earth Surface Processes and Landforms* **37**: 572–582.

Whited DC, Lorang MS, Harner MJ, Hauer FR, Kimball JS, Stanford JA. 2007. Climate, hydrologic disturbance, and succession: drivers of floodplain pattern. *Ecology* **88**: 940–953.

Wohl E, Bledsoe BP, Jacobson RB, Poff LR, Rathburn SL, Walters DM, Wilcox AC. 2015a. The natural sediment regime in rivers: broadening the foundation for ecosystem management. *Bioscience* **65**: 358–371.

Wohl E, Lane SN, Wilcox AC. 2015b. The science and practice of river restoration. *Water Resources Research* **51**: 5974–5997.

Supporting Information

Additional supporting information may be found online in the Supporting Information section at the end of the article.

Data S1 Supporting Information

© 2020 John Wiley & Sons, Ltd.